Journal of Materials Chemistry B

Accepted Manuscript

ROYAL SOCIETY OF CHEMISTRY

www.rsc.org/materialsB

Journal Name

RSCPublishing

ARTICLE

Site-selective biomineralization of native biological membranes

Cite this: DOI: 10.1039/x0xx00000x

Annegret P. Busch[a], Daniel Rhinow[b], Fang Yang[a], Hendrik Reinhardt[a], André Beyer[c], Armin, Gölzhäuser[c], Norbert Hampp[a,d]

Received 00th January 2012,
Accepted 00th January 2012

DOI: 10.1039/x0xx00000x

www.rsc.org/

Biomineralization of silica precursors, mediated by self-assembled proteins, is performed by many organisms. The silica cell walls of diatoms are perhaps the most stunning biomineral structures. Although the mechanisms of biomineralization are still not fully understood, template-assisted formation of silica nanostructures has gained much attention in the materials science community. Precise control of the location and the shape of structures obtained by biomineralization remains a challenge. This paper introduces a versatile biotechnological process that enables site-selective biomineralization of native biological membranes using genetically modified purple membrane (PM) from *Halobacterium salinarum* as a template. PM is a two-dimensional crystal consisting of bacteriorhodopsin (BR) and lipids. In this work we study PM-E234R7, a genetically modified PM containing mutated BR, where seven amino acids, starting from E234, were replaced by arginine in the C-terminus. The arginine sequence catalyzes silica formation from a tetraethylorthosilicate (TEOS) precursor. Silification of the mutated PM variant starts with initial formation of membrane-attached spherical silica nanoparticles, which then fuse to form 2D silica nanoflakes, selectively, on the cytoplasmic side of the PM. Genetical modification of membrane proteins with poly-arginine sequences may be a general route for site-selective biomineralization of native biological membranes.

Introduction

Template-assisted biomineralization of inorganic precursors enables organisms to build a variety of well-defined nanostructures, such as bones, teeth, and diatoms.[1-12] Some organisms use silica as a construction material, e.g. diatoms, radiolarian, synophytes as well as multicellular sponges, and some plants like rice.[10] Diatoms are the most prominent examples of biological structures obtained by silification. Their skeletons are tough structures generated from silica precursors by catalysis of amine-rich peptide sequences, referred to as silaffins.[1,2] Silaffins are proteins post-translationally modified with long-chain oligo-N-methly-propylamines. They were identified as the main organic components of diatom biosilica.[1] *In vitro* studies have demonstrated that silaffins induce polycondensation of silicic acid under physiological conditions and also act as a framework for silica biomineralization.[1,2,13-15] Bio-inspired silicification of suitable templates has been studied by many research groups.[3,4,16-20] Only a few studies reported silicification of biological membranes.[17,21,22] Most studies refer to conditions where membranes, organelles or whole cells are nonspecifically entrapped in a silica matrix to protect the biomaterial from environmental stress.[17,22-24] However, building functional biohybrid devices from silicified membranes requires site-selective biomineralization. It is known that small cationic peptides facilitate nucleation of silica precursors.[16,20] In this work we study site-selective silicification of a genetically modified variant of the purple membrane (PM) from *Halobacterium salinarum.* PM is a native two-dimensional (2D) crystal consisting of the integral membrane protein bacteriorhodopsin (BR) and lipids only.[25,26] The 20-amino acid long C-terminus, located at the cytoplasmic side of the membrane, is easily modified by genetic tools and interacts freely with the surrounding medium. We demonstrate that substituting 7 cytoplasmic amino acids, starting from E234, by seven arginines converts PM into a template with densely packed cationic residues enabling selective silicification of the cytoplasmic side of PM-E234R7. Biomineralization of PM-234R7 is studied by a variety of physical techniques. Micrometer-scaled PM-E234R7 patches represent a perfectly ordered nano-patterned array of functional groups suitable as templates for directed silicification. Inserting poly-arginine sequences in the C-terminus of membrane proteins may be a general approach to accomplish site-selective silicification of biological membranes.

Experimental

Materials

Chemicals were purchased from Sigma-Aldrich (Taufkirchen, Germany), Fisher Scientific (Leicestershire, United Kingdom), and Fluka (Buchs, Switzerland) and were used as received.
Mica and highly oriented pyrolytic graphite (HOPG) substrates for the AFM/EFM experiments were purchased from Plano (Wetzlar, Germany). Both substrates were extensively washed with doubly distilled water before use.

Preparation of PM

PM variant PM-E234R7 was prepared as described earlier.[27] Purified PM-E234R7 was lyophilized and stored at -20 °C until further use.

UV/Vis spectroscopy

UV/Vis absorption spectra of light-adapted BR were recorded on a Lambda 35 spectrometer (PerkinElmer Instruments, USA). Spectra were normalized to an optical density (OD) = 0 at 800 nm to compensate for scattering effects.

General procedure for silicification of PM-E234R7

Experiments were carried out in 10 mM ethylamine-citrate buffer of pH = 5. PM was suspended in 3 ml of the reaction buffer and tetraethylorthosilicate (TEOS) was carefully added within 5 -10 minutes until the desired ratio was obtained. The concentration of PM was measured by UV/Vis spectroscopy, using a decadic molar extinction coefficient of ε_{570nm} = 63,000 mol l^{-1}·cm^{-1}. TEOS was added relative to the molar amount of PM in the sample ranging from 0.2 to 10.0 equivalents. BR-E234R7 has a molar mass of 27281 Da. The molar mass of BR-E234R7 and TEOS is 27.172 g mol^{-1} and 208.32 g mol^{-1}, respectively. Addition of 1 molar equivalent of TEOS means that 7.66 µg of TEOS were added per mg of PM-E234R7. After 24 h of incubation at 4°C under slight agitation, silicified PM was removed from the solution by centrifugation (15 min, 13,000 rpm, room temperature, Biofuge 13, Heraeus) and suspended in water. The silicified material was stored in suspension at -20°C until further use.

Analytical density gradient centrifugation

The buoyant density of silicified PM-E234R7 was analyzed by ultracentrifugation on a five-step sucrose density gradient. (D+)-sucrose solutions with concentrations of 39 %, 41%, 50 %, 55 %, and 60 % were used. Starting with the highest density, 2.2 mL of each solution was funneled into an ultra-centrifugation tube (12.5 mL; Kontron 9091-90200) by a peristaltic pump to form density layers. 200 µL of PM material (PM-E234R7: OD_{570} = 21, silicified PM-E234R7: OD_{570} = 18) were placed onto sucrose density gradients, tared with Millipore water and were centrifuged in a Sorvall® WX ultra 80 centrifuge in a Sorvall® Surespin 630/36 rotor at 4°C and 25,000 rpm for 19 h.

Determination of zeta potential

The zeta potential was measured with a Delsa™ Nano C particle analyzer (BeckmanCoulter). For these measurements suspensions of PM-E234R7 and silificated PM-E234R7 (each OD = 10) in Millipore water were used.

Transmission electron microscopy

Silicified PM-E234R7 was analyzed in a FEI Tecnai Polara microscope operating at 300 kV, equipped with a post-column energy filter and a 2k x 2k CCD camera (Gatan). Elemental maps were obtained using the three-window method. Si maps were acquired at the Si L edge (119 eV, slit width 20 eV, 20 s acquisition time), S maps were acquired at the S L edge (180 eV, slit width 20 eV, 40 sec acquisition time).

Scanning electron microscopy (SEM)

Silicified PM-E234R7 was suspended in distilled water and dropped onto carbon coated copper grids (Plano, Wetzlar, Germany). SEM analysis was performed using a JEOL JSM-7500F SEM. Energy dispersive X-ray spectroscopy (EDX) was done with a CamScan CS 4 SEM operated at 20 keV. For this purpose the samples were trickled on carbon-coated copper grids and fixed on aluminium SEM sample holders with conductive tabs (both Plano, Wetzlar, Germany).

Helium Ion Microscopy (HIM)

Silicified PM-E234R7 was suspended in distilled water and dripped on stainless steel carriers. Helium Ion Microscopy (HIM) was done with a Carl Zeiss Orion Plus. The helium ion beam was operated at 30 kV acceleration voltage at a current of 0.5 pA. A 10 µm aperture at spot control 5 was used. Secondary electrons were collected by an Everhart-Thornley detector at 500 V grid voltage. The working distance was about 10 mm. A dwell time per pixel of 2 µs at 16 lines averaging was used. All HIM micrographs were recorded with a pixel size of 0.49 nm.

Atomic force microscopy (AFM)

Tapping mode (TM) atomic force microscopy (AFM) was chosen for topological imaging. Imaging was performed in liquid with a Nanoscope IV system (Veeco, Santa Barbara, CA). Images were acquired using TM-AFM with constant amplitude attenuation. The cantilever approach (Silicon-tip on nitride cantilever, k = 0.32 N/m, f = 40-75 kHz) was performed with an initial drive amplitude of 0.499 V (tip oscillation amplitude 1.5 V). Electrostatic force microscopy (EFM) was conducted in air using SCM-PIT tips (antimony (n) doped Si, k = 1 - 5 N/m, f_0= 70 - 83 kHz, 0.01 – 0.025 Ω/cm, Veeco, Santa Barbara, CA) and utilizing the Nanoscope´s LiftMode feature.

Results and Discussion

In this work BR-E234R7 molecules, bearing a hepta-Arg (Scheme 1) sequence in the C-terminus, serve as a template for selective biomineralization of the cytoplasmic side of PM-E234R7.

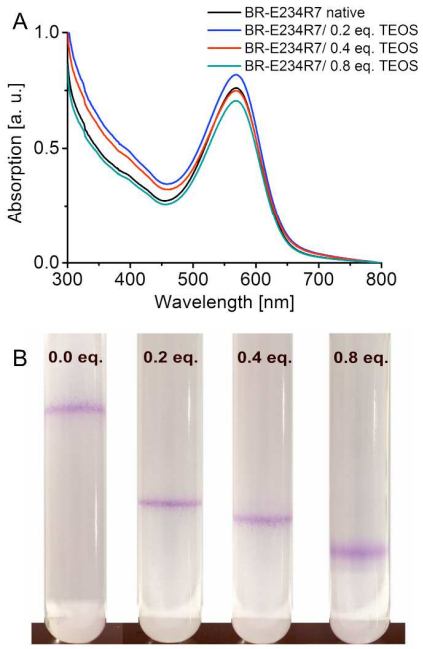

Figure 1. Physico-chemical properties of purple membrane PM-E234R7 in dependence on the degree of silicification. (A) The absorption spectra of silicified PM-E234R7 show a maximum at 570 nm indicating preservation of the retinal chromophore. (B) Density gradient centrifugation of native (0.0 eq.) and silificated PM, i.e. 0.2 eq., 0.4 eq., and 0.8 eq. of TEOS. All materials show sharp bands but with significantly different buoyant densities caused by the increasing amount of nano-silica formed on the cytoplasmic side.

The buffer system contains ethylamine which acts as a stabilizing agent for the initially formed polysilicic acid or silica nanoparticles, thus preventing uncontrolled aggregation of primary silica in solution.[17] In this buffer system, neither visible aggregation nor gel-formation occurs for more than one day in the presence of the silicic acid precursor tetraethylorthosilicate (TEOS) without PM-E234R7. The silicification of PM-E234R7 has no effect on the absorption spectrum (Figure 1A) indicating that the BR chromophore is preserved. Analytical sucrose density gradients of PM-E234R7 before and after silicification to various degrees, are shown in Figure 1B. The buoyant density of PM-E234R7 increases with increasing ratios of TEOS/PM.

Zeta potentials of silicified PM-E234R7 were measured by dynamic light scattering (DLS). The zeta potential of PM-E234R7 is -39.6 mV, significantly more positive than that of wild-type PM, which has a zeta potential of -52 mV.[28] This difference can be attributed to the genetically introduced hepta-Arg sequence. With increasing amounts of TEOS equivalents, the zeta potential of PM-E234R7 decreases proportionally, indicating increasing silicification (Table 1). Increasing silicification causes neutralization of the positively charged hepta-Arg sequence by negatively charged silica nanoparticles.

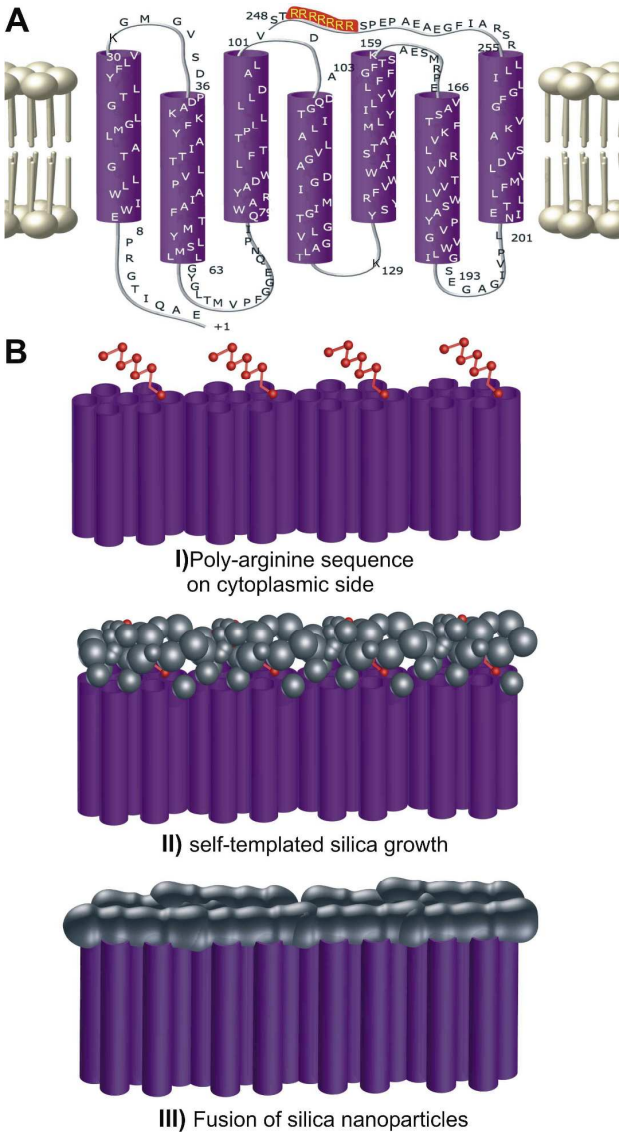

Scheme 1: PM-E234R7 as a template for site-selective biomineralization. (A) In the cytoplasmatic C-terminus of wild-type PM, a sequence of amino acids, geginning with E234, was replaced by seven arginine residues (red). This renders the cytoplasmic side of PM positively charged. (B) I) – III) Densely packed poly-arginine sequences in PM-E234R7 serve as a template for the formation silica nanoparticles. Ripening of the silica layer leads to a dense nanosized silica layer.

PM mutant / eq. TEOS	Zeta potential [mV]	Si EDX (1.74 keV) [counts]
E234R7 native	-39.6	-
E234R7 / 0.2	-50.3	1578
E234R7 / 0.4	-55.7	3725
E234R7 / 0.8	-61.0	6614

Table 1 Physico-chemical properties of silicified PM-E234R7. (middle column) The Zeta potential of PM-E234R7 decreases with increasing silicification (right column) EDX signal of silicon acquired from silicified PM-E234R7.

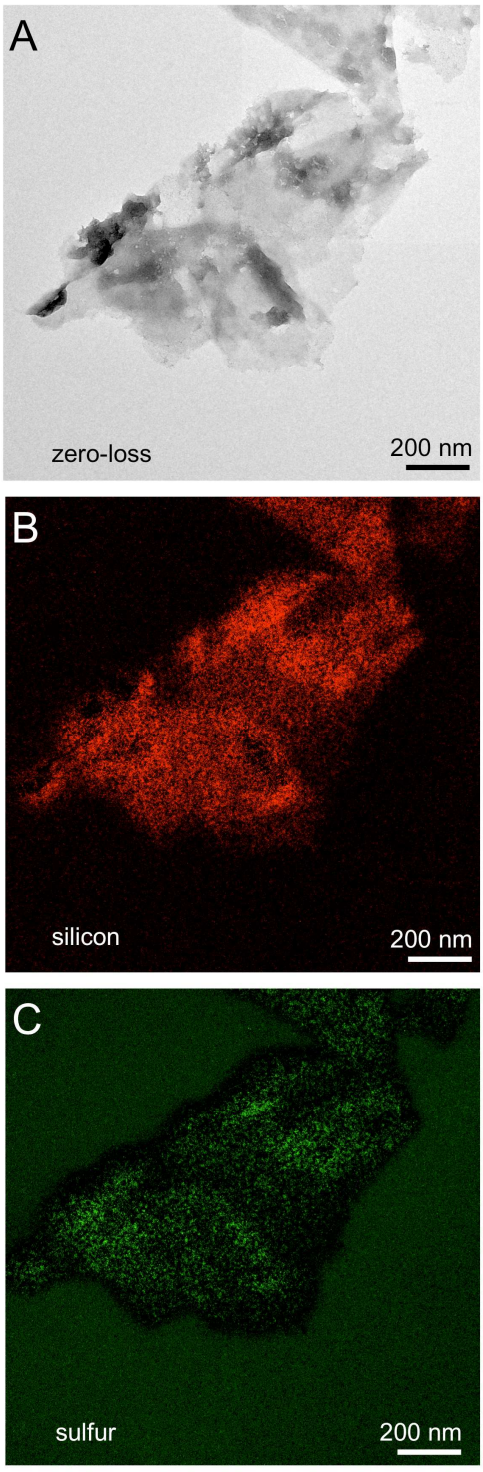

Figure 2 Energy-filtered TEM analysis of silicified PM-E234R7 (a) Zero-loss TEM image of a single silicified PM. (b) Silicon map of the same PM. (c) Sulfur map of the same PM. The sulfur signal is generated by sulfur-containing amino acids in BR. Owing to the strong absorption of the silica layer, the background of the support film appears brighter than the membrane rims.

To analyze silicification of PM-E234R7 at the level of single membranes we performed energy-filtered transmission electron microscopy (EFTEM) of biomineralized PM-E234R7. Fig. 2A shows a zero-loss EFTEM image of silicified PM-E234R7. Elemental maps acquired from the same PM confirm that PM-E234R7 is covered with silica (Fig. 2b). Fig. 2c demonstrates that the lateral size of the silica nanolayer, covering PM-E234R7, exceeds the size of the PM patch.

Scanning electron microscopy (SEM) was used to analyze the morphology of silica formed on PM-patches as a function of TEOS equivalents in detail (Figure 3). While secondary electrons (SE) primarily give information about the topology of the sample, backscattered electrons (BSE) are particularly sensitive to the atomic number and give information about the silica distribution. Superposition of both detector images (SE = green, BSE = red) shows how the amount of silica attached to the PM patches increases in dependence of TEOS equivalents (Fig. 3). Initially, silicification leads to formation of nanosized silica spheres, which later fuse into nanoscaled silica flakes attached to the cytoplasmic side of PM (Scheme 1). Upon incubation with 0.8 eq. TEOS, the surface of PM-E234R7 is completely covered. In addition, the degree of silicification was monitored by energy dispersive X-ray spectroscopy (EDX) (Table 1).

To analyze silicified PM-234R7 under near-native conditions, we used tapping mode atomic force microscopy (TM-AFM) in liquid. Figure 4 shows PM-E234R7 samples, silicified with 0.2 and 0.8 eq. of TEOS. On top of the PM spherical silica particles, attached to the surface, are observed. Their height is about 5 nm as derived from the cross-sections taken from AFM images of the 0.2 eq. sample. We used electrostatic force microscopy (EFM) to confirm that silica nanoparticles are attached to the cytoplasmic site of PM-E234R7 (not shown). With increasing TEOS concentrations the silica nanoparticles fuse into small nanoflakes (Figure 4, right). With increasing silicification the height of the silica nanoparticles remains unchanged, whereas their lateral dimensions increase significantly. We observed silica nanoflakes with lateral dimensions up to 76 nm (Fig. 4, right). The initially formed spherical silicate nanoparticles fuse into extended silica nanoflakes (Scheme 1). In reference experiments with wild-type PM no silica nanoparticles were found attached to the PM surface (see Figure 5 and Supplementary Information, Figure S1) proving that the introduced poly-arginine sequence in PM-E234R7 is responsible for the observed biomineralization. It is known from former experiments that cationic polymers are needed to induce silica formation on wild-type PM.[17]

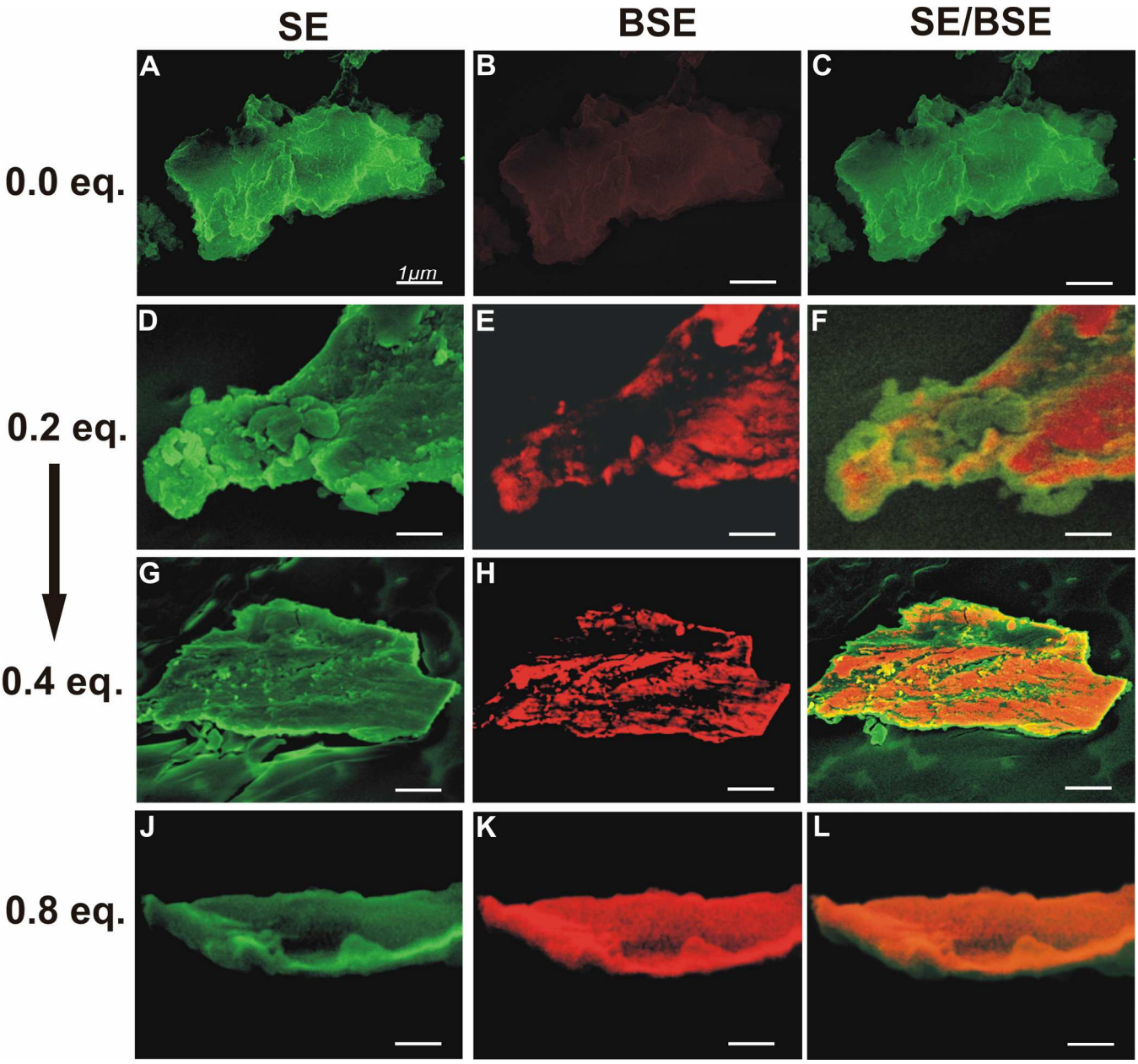

Figure 3. Gradual silicification of PM-E234R7. Characterization of the hybrid material consisting of PM and attached silica by scanning electron microscopy (SEM). From top to bottom the ratio of TEOS added to the PM is increased. In the left column, the morphology of the samples is seen as a secondary electron (SE) image shown in green. The middle column shows the corresponding backscattered electron (BSE) images in red, which reflect mainly the silica distribution. The right column shows the superposition of the SE and BSE images. With increasing amount of TEOS added, a proportionally higher degree of silicification is observed.

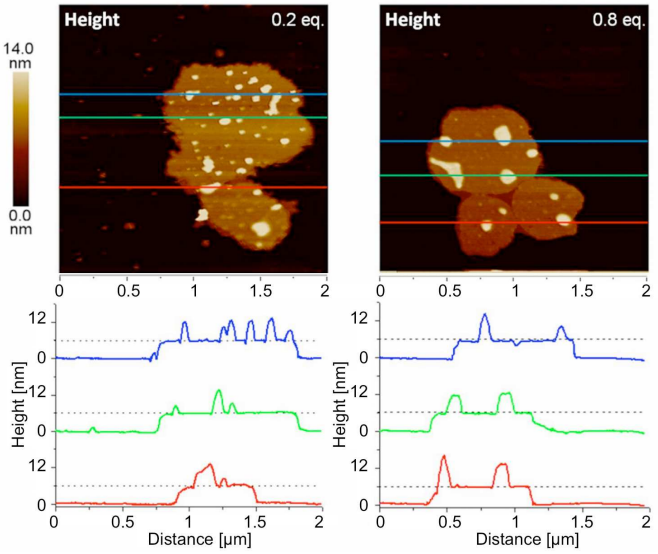

Figure 4. Topography of PM-E234R7 analyzed by AFM. (left) TM-AFM height images of PM-E234R7 with attached silica nanoparticles (0.2 eq.) on mica acquired in liquid. (right) At higher TEOS concentrations, e.g. 0.8 eq., the silica nanoparticles fuse into small islands attached to the PM patches.

We analyzed the surface of biomineralized PM-E234R7 using helium ion microscopy (HIM). We have chosen HIM to show that biomineralization occurs on one side only. SEM is not a suitable tool for this task, as the low contrast of the purple membrane does not allow to analyze on which side of the purple membrane the silica particles are located. A particular advantage of HIM is that it provides high chemical contrast for light elements making it ideal to study the structure of biohybrid materials such as silicified PM-E234R7.[29] Fig. 6 shows SE HIM images of silicified PM-E234R7. For the sake of clarity the silica particles are colored in orange and the membranes are colored in green. The only difference between PM-WT and PM-E234R7 is the replacement of amino acids in the N-terminal sequence for arginine. Biomineralization is observed with the mutated protein and not at all with PM-WT. Obviously the introduced mutation is responsible for the changed properties and the biomineralization occurs where the arginines are introduced. The HIM images confirm the model proposed in Scheme 1. First, isolated silica nanoparticles are formed, which then fuse into small 'nano-islands' (Fig. 6A), and finally form a silica flake on the PM surface (Fig. 6B). The sample shown in Figure 6B belongs to a membrane preparation, incubated with a 10-fold excess of TEOS. As a result, a silica nanoflake is observed, which is selectively formed on the cytoplasmic side of the membrane where the hepta-Arg sequences are exposed to the medium. The HIM image (Fig. 6B) shows the extracellular side of a silicified PM-E234R7, which is virtually free of any silica. Interestingly, the lateral dimensions of the silica flake exceed the size of the PM, thus resembling observations made by EFTEM (Fig. 2c).

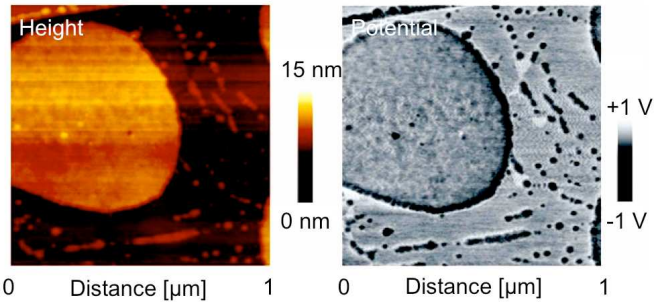

Figure 5. Control experiments with PM-Wildtype. Silicification experiments were performed with 0.4 eq. TEOS. (left) Topography of wild-type PM on highly oriented pyrolytic graphite (HOPG). (right) EFM images showing negatively charged silica nanoparticles in the vicinity of wild-type PM but not on the PM.

Conclusions

We have shown that genetical modification of integral membrane proteins enables site-selective biomineralization of native biological membranes. Polyarginine-catalyzed templated silica-biomineralization was demonstrated using PM-E234R7, a mutated purple membrane from *Halobacterium salinarum*. A hepta-arginine sequence was cloned into the C-terminus at the cytoplasmic side of PM enabling selective silicification of the cytoplasmic side of the membrane. The biosilification process was analyzed using electron and ion microscopy as well as atomic force microscopy. It was found that with increasing availability of the inorganic precursor TEOS the initially formed silica nanoparticles fuse into extended nanoflakes on the PM until it is covered with a dense layer. Poly-arginine sequences can easily be introduced in any membrane protein enabling site-selective silicification. Asymmetrically silicified biomembranes might find application as building blocks for nanobiotechnology. Furthermore, the process enables precise control over the accessibility and activity of the sides of biological membranes.

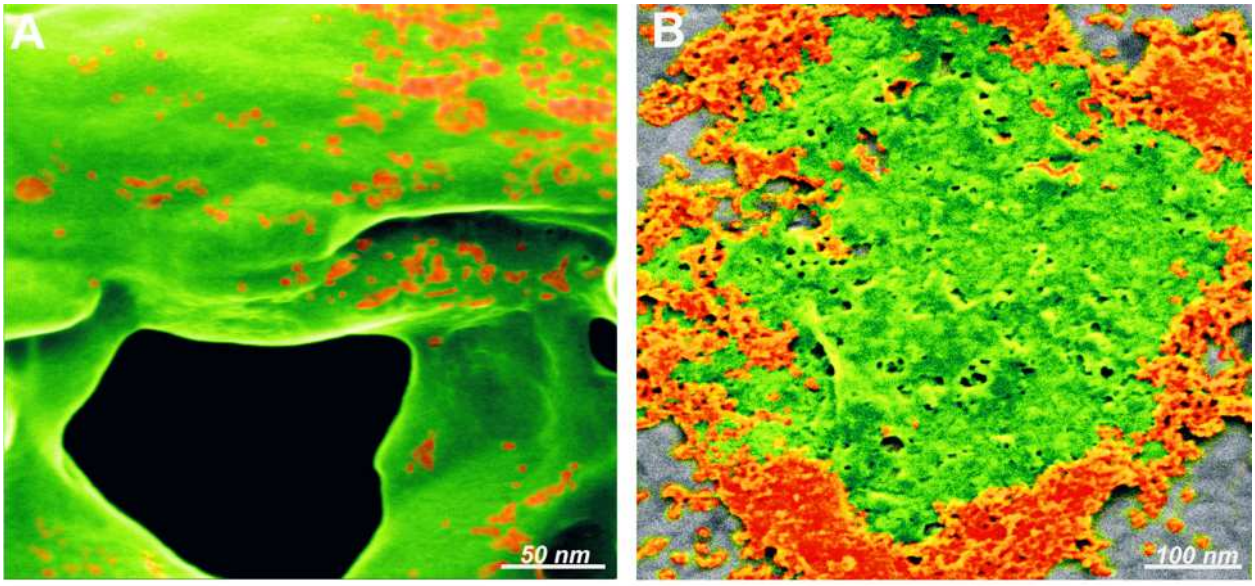

Figure 6. Helium ion microscopy of silicified PM-E234R7. (A) PM-E234R7 silicified with 0.2 eq. TEOS (B) PM-E234E7 silicified with 10.0 eq. TEOS imaged from the extracellular side. A layer of fused silica nanoparticles (orange) is attached to the cytoplasmic side of PM-E234R7 (green).

Acknowledgements

We thank Nina Schneider for preparation and purification of the PM variant, PM-E234R7. Financial support by the German Ministry of Education and Research (BMBF), through grant B-Safe plus (FKZ13N9541) is gratefully acknowledged.

Notes and references

[a] University of Marburg, Department of Chemistry, Hans-Meerwein-Str., 35032 Marburg, Germany.
[b] Max Planck Institute of Biophysics, Department of Structural Biology, 60438 Frankfurt, Germany.
[c] University of Bielefeld, Department of Physics, 33501 Bielefeld, Germany.
[d] Material Science Center, 35032 Marburg, Germany.

1 N. Kröger, R. Deutzmann and M. Sumper, *Science*, 1999, **286**, 1129.
2 M. Sumper and N. Kröger, *J. Mater. Chem.*, 2004, **14**, 2059.
3 S. Mann, *Angew. Chem. Int. Ed.,* 2000, **39**, 3392.
4 M. B. Dickerson, K. H. Sandhage and R. R. Naik, *Chem. Rev*., 2008, **108**, 4935.
5 V. C. Sundar, A. D. Yablon, J. L. Grazul, M. Ilan and J. Aizenberg, *Nature*, 2003, **424**, 899.
6 Y. Politi, T. Arad, E. Klein, S. Weiner and L. Addadi, *Science*, 2004, **306**, 1161.
7 J. Aizenberg and G. Hendlen, *J. Mater. Chem*, 2004, **14**, 2066.
8 J. Aizenberg, J. C. Weaver, M. S. Thanawala, V. C. Sundar, D. E. Morse and P. Fratzl, *Science*, 2005, **309**, 275–278.
9 J. Aizenberg, V. C. Sundar, A. D. Yablon, J. C. Weaver and G. Chen, *Proc. Natl. Acad. Sci*, 2004, **101**, 3358.
10 M. Hildebrand, Diatoms, Biomineralization Processes, and Genomics, *Chem. Rev.*, 2008, **108**, 4855.
11 L. Addadi, S. Raz and S. Weiner, *Adv. Mater.*, 2003, **15**, 959.
12 A. Veis, *Science*, 2005, **307**, 1419.
13 F. Noll, M. Sumper and N. Hampp, *Nano Lett.*, 2002, **2**, 91.
14 H. R. Luckarift, J. C. Spain, R. R. Naik and M. Stone, *Nat. Biotechnol.*, 2004, **22**, 211.
15 H. Menzel, S. Hostmann, P. Behrens, P. Bärnreuther, I. Krueger and M. Jahns, *Chem. Commun.*, 2003, **24**, 2994.
16 J. N. Cha, G. D. Stucky, D. E. Morse. and T. J. Deming, *Nature*, 2000, **403**, 289.
17 A. Schönafinger, S. Müller, F. Noll, N. Hampp, *Soft Matter* 2008, **4**, 1249.
18 J. H. Moon, J. S. Seo, Y. Xu and S. Yang, *J. Mater Sci.* 2009, **19**, 4687.
19 C. Y. Khripin, D. Pristinski, D. R. Dunphy, C. J. Brinker and B. Kaehr, *ACS Nano* 2011, **5**, 1401.
20 J. P. Hinestrosa, J. E. Sutton, D. P. Allison, M. J. Doktycz, J. M. Messman and S. T. Retterer, *Langmuir* 2013, **29**, 2193.
21 A. Bernecker, J. Ziomkowska, S. Heitmüller, R. Wieneke, A. Geyer and C. Steinem, *Langmuir* 2010, **26**, 13422.
22 R. Esquembre, S. N. Pinto, J. A. Poveda, M. Prieto and C. R. Maeto, *Soft Matter*, 2012, **8**, 408.
23 C. F. Meunier, P. van Cutsem, Y.-U. Kwon and B.-L. Su, *J. Mater. Chem.*, 2009, **19**, 1535.
24 A. Collins, D. Rhinow, N. Hampp and S. Mann, *Biomacromolecules*, 2009, **10**, 2767.
25 D. Oesterhelt and W. Stoeckenius, *Nat. New Biol.*, 1971, **233**, 149.
26 U. Haupts, J. Tittor and D. Oesterhelt, *Annu. Rev. Biophy. Biomol. Struct.*, 1999, **28**, 367.
27 R.-P. Baumann, A. P. Busch, B. Heidel and N. Hampp, *J. Phys. Chem. B*, 2012**, 116**, 4134.
28 K. C. Ng and L.-K. Chu *J. Phys. Chem B*, 2013, **117**, 6241.
29 D. C. Bell, *Microsc. Microanal.* 2009, **15**, 147.

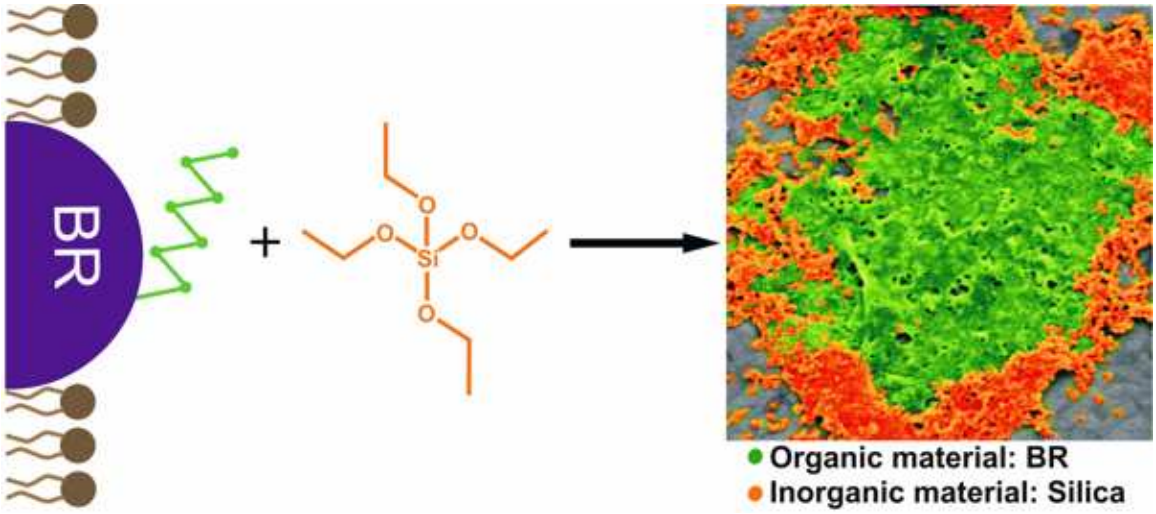

Genetical modification of integral membrane proteins with poly-arginine sequences enables site-selective silicification of a native biological membrane.